Furthermore, the transformation matrix of Δ of the canonical form is obtained as,

$$\Delta = \mathcal{Q}_O(\mathcal{H})^{-1}\bar{\mathcal{Q}}_O \tag{27}$$

The error dynamics of the system in the form of observer canonical form is denoted as Γ, for which

$$\Gamma = A_o - \Psi_o C_o \longrightarrow \Psi_o = \begin{bmatrix} l_1 \\ l_2 \\ l_3 \end{bmatrix} \tag{28}$$

and the characteristic polynomial of Γ is $\det(sI - \Gamma)$. Proposing a new matrix of Γ_d with the desired eigenvalues of λ_i for $i = 1, \ldots, n$ with n equals to the number of full rank of A. From this, the polynomial of Γ should be compared to that of Γ_d with certain λ_i and the value of Ψ_o is then obtained. Lastly, the gain of the observer is given by,

$$\Psi = \Delta\Psi_o \tag{29}$$

and the matrix showing the dynamic of the system is written by $\Gamma_d = A - \Psi C$.

D. Adaptive-Scaling Kalman Filter

The idea of the term "scaling" is proposed in [16] which is then further modified in [17]. The following is the prediction of a dynamic system in discrete time,

$$\hat{x}_{k|k-1} = A_k\hat{x}_{k-1|k-1} + B_k\vartheta_k \tag{30}$$

$$\hat{y}_k = \Theta_k\hat{x}_{k|k-1} + \chi_k \tag{31}$$

where $\hat{y}_k \in \mathbb{R}^p$ as measurements whereas ϑ_k and χ_k are set as $\mathcal{WGN}$ such that $\mathbf{E}(\vartheta_k\vartheta_l^\top) = Q_k\Omega$ and $\mathbf{E}(\chi_k\chi_l^\top) = R_k\Omega$. x_0 is defined as the initial state with $x_0 = \mathcal{N}(\bar{x}_0, P_0)$. Given the set of measurements $Y_k = [y_0, y_1, \ldots, y_k]$. From those, the covariance matrices of prediction in Kalman are then set as given

$$P_{k+1} = AP_kA^\top + \phi_k B_k Q_k B_k^\top \tag{32}$$

$$\begin{aligned}\bar{P} &= \Theta P_{k+1}\Theta^\top + R_k \\ &= \Theta AP_kA^\top\Theta^\top + R_k + \phi_k\Theta B_kQ_kB_k^\top\Theta^\top\end{aligned} \tag{33}$$

where ϕ_k is what is called as scaling parameter as a modification of covariance matrices. Let $\nu_k = y_k - \hat{y}_{k|k-1}$ and, a-priori, the result of the $(\nu_k)^2$ being showed as $|\nu_k|^2 = \nu^\top\nu$ is supposed to be the diagonal elements of $\bar{P}$ consisting the scaling variable ϕ. For the simplification, by introducing new variables $\alpha_\theta, \beta_\theta, \gamma_\theta$, the Eq. (33) can be written as follows,

$$\alpha_\theta = \bar{P} \tag{34a}$$

$$\beta_\theta = \Theta AP_kA^\top\Theta^\top + R_k \tag{34b}$$

$$\gamma_\theta = \phi_k\Theta B_kQ_kB_k^\top\Theta^\top \tag{34c}$$

such that,

$$\alpha_\theta = \beta_\theta + \gamma_\theta \tag{35}$$

To obtain ϕ, by proposing some new constants of a, b, c with $a \geq 0, b \geq 0, c \geq 0$ and $a + b + c = 1$, it is given by

$$\Upsilon_k = a\phi_0 + b\phi_{k-1} + c\left[\frac{\nu_k - (\beta_\theta)_k}{(\gamma_\theta)_k}\right] \tag{36}$$

where $\phi_k = \max(\Upsilon_k, 0)$ and $\phi_0 = 1$ at $k = 0$. if $|\nu_k|^2 = \alpha_\theta$,

$$\Upsilon_k = a\phi_0 + (b + c)\phi_{k-1} \tag{37}$$

$$\phi_k = \max(\Upsilon_k, 0) \tag{38}$$

The updates of the estimated states and covariance matrices are presented in the following,

$$K_k = P_{k|k-1}\Theta^\top\bar{P}^{-1} \tag{39}$$

$$\hat{x}_{k|k} = \hat{x}_{k|k-1} + K_k\nu_k \tag{40}$$

$$P_{k|k} = (I - K_k\Theta)P_{k|k-1} \tag{41}$$

Keep in mind that the this linear system could be switched into non-linear system as it is an adaptive-scaling Kalman filtering.

E. Consensus Filtering

From [18] and [19] and recalling Eqs. (30) and (31) using the same scenarios of initial condition of covariance matrices Q_k, R_k, x_0 with the same dimensional definition of Y_k and ν_k, the state estimates could be written as,

$$\begin{aligned}\hat{x}_k &= \mathbf{E}(x_k|Y_k), & \bar{x}_k &= \mathbf{E}(x_k|Y_{k-1}) \\ P_k &= \sum(k+1|k), & \mathcal{P}_k &= \sum(k+1)\end{aligned} \tag{42}$$

where P_k as initial state of error covariance. That P_k and the inverse of covariance matrix H_k with certain number of sensors communicated as distributed large-scale system are paired to generate matrix $\mathcal{P}_k$, such that

$$H_k = \frac{1}{n}\sum_{i=1}^{n}\left(\Theta_k^\top R_k^{-1}\Theta_k\right)_i \tag{43}$$

$$\mathcal{P}_k^{-1} = (nP)^{-1} + H_k \tag{44}$$

whilst matrix of K is affected by the matrix of $\mathcal{P}$ as given,

$$K = \mathcal{P}_k\Theta_k^\top R_k^{-1} \tag{45}$$

The updates of the state estimation is formulated as follows:

$$\hat{x}_k = \hat{x}_{k|k-1} + K\left(y_k - \Theta\hat{x}_{k|k-1}\right) \tag{46}$$

$$= \hat{x}_{k|k-1} + \mathcal{P}_k(\Theta_k^\top R_k^{-1}y_k - \Theta_k^\top R_k^{-1}\Theta\hat{x}_{k|k-1}) \tag{47}$$

from the equation, it can be simplified by introducing z_k which is also affected by some n sensors, if any, and a new measurement is written as

$$z_k = \frac{1}{n}\sum_{i=1}^{n}\Theta_k^\top R_k^{-1}y_k \tag{48}$$

$$\hat{x}_m = \bar{x} + \mathcal{P}_k(z_k - H_k\bar{x}) \tag{49}$$

compared to the classic Kalman filter, the prediction of $\hat{x}$ and P are becoming the update of this μKF such that:

$$P_k^+ = A\mathcal{P}_kA^\top + BQ_kB^\top \tag{50}$$

$$\bar{x}^+ = A\hat{x}_m \tag{51}$$

This algorithm has some pros in terms of simplifying a huge calculation in conventional-KF which is not feasible. While it is required some additional high-, low-, and band-pass filter in tackling consensus dynamic problems, for this paper, it is only halt in Eq. (51). This method is comparable as another modified algorithm from the original KF and they are observed in terms of the capability in estimating the unhealthy system.

http://dx.doi.org/10.29322/IJSRP.11.05.2021.p11308

Algorithm 1 Adaptive-Scaling and Consensus Filtering

Initialization:
$x_0 \sim \mathcal{N}(\bar{x}_0, P_0)$; $q \sim \mathcal{N}(\bar{q}, \Psi_q)$;
R_k, Q_k, $Y_k = [y_0 \to y_k]$, α_θ, β_θ, γ_θ, ϕ_k, z_k;
$x_0 = \bar{x}_0$ and $P_0 = \Psi_x$
for $i = 1$ to κ **do**
  for $k = 1$ to N **do**
    1. Adaptive-Scaling Kalman:

$$\hat{x}_{k|k-1} = A_k \hat{x}_{k-1|k-1} + B_k \vartheta_k$$
$$\hat{y}_k = \Theta_k \hat{x}_{k|k-1} + \chi_k$$
$$\alpha_\theta = \beta_\theta + \gamma_\theta$$
$$\Upsilon_k = \begin{cases} a\phi_0 + b\phi_{k-1} + c\left[\frac{\nu_k - (\beta_\theta)_k}{(\gamma_\theta)_k}\right], \text{otherwise} \\ a\phi_0 + (b+c)\phi_{k-1}, \text{if } |\nu_k|^2 = \alpha_\theta \end{cases}$$
$$\phi_k = \max(\Upsilon_k, 0)$$
$$K_k = P_{k|k-1}\Theta^\top \bar{P}^{-1}$$
$$\hat{x}_{k|k} = \hat{x}_{k|k-1} + K_k \nu_k$$
$$P_{k|k} = (I - K_k\Theta)P_{k|k-1}$$

    2. *Consensus*-Filtering:

$$H_k = \Theta_k^\top R_k^{-1} \Theta_k$$
$$\mathcal{P}_k = (P^{-1} + H_k)^{-1}$$
$$z_k = \Theta_k^\top R_k^{-1} y_k$$
$$\hat{x}_m = \bar{x}_0 + \mathcal{P}_k(\hat{z}_k - H_k \bar{x}_0)$$
$$P_k^+ = A\mathcal{P}_k A^\top + BQ_k B^\top$$
$$\bar{x}^+ = A\hat{x}_m$$

    Collecting Estimation Error:

$$e_1 = |x_k - \hat{x}_k|$$
$$e_2 = |x_k - \bar{x}_k^+|$$

  end for
end for

F. Fault Detection Scheme

This subsection is initiated by computing the output residual which is then defined as,

$$\varepsilon(t) = Ce(t) \longrightarrow e(t) = \mathcal{L}^{-1}\left[(sI - \Gamma_d)^{-1}\right] e(0) \tag{52}$$

where $e(t)$ is the state estimation error being described as $e(t) = x(t) - \hat{x}(t)$ and its dynamics is denoted as $\dot{e}(t) = \Gamma_d e(t)$. The fault detection scheme is supposedly detected at time $t_d > t_f$, satisfying $\varepsilon(t_d) > \bar{\varepsilon}(t_d)$ with

$$\bar{\varepsilon}(t) = C\mathcal{L}^{-1}\left[(sI - \Gamma_d)^{-1}\right]\hat{e} \longrightarrow \hat{e} = \begin{bmatrix} \hat{e}_1 \\ \hat{e}_2 \\ \hat{e}_3 \end{bmatrix} \tag{53}$$

where $\bar{\varepsilon}$ is the designed appropriate threshold with some initial ranges of $x_i(0)$ for $i = 1, \ldots, n$ allowing to detect the fault f in a finite time $t_d > t_f$. Observing that $\varepsilon(t) \to 0$, $\forall t \to \infty$, it can be said that for $t \geq t_f, \exists t_d > t_f \coloneqq \varepsilon(t_d) > \bar{\varepsilon}(t_d)$.

III. Numerical Results

The design of the simulation is shown with the following variables so that $\psi_1 = 2$, $\psi_2 = 1$, $\psi_3 = 2$ and $\delta_1 = 1$, $\delta_2 = 1.5$, $\delta_3 = 1$. From these, the state space system is,

$$\dot{x} = \overbrace{\begin{bmatrix} -0.5 & 0.0 & 0.0 \\ 0.5 & -1.5 - \bar{\delta} & 0.0 \\ 0.0 & 1.5 & -0.5 \end{bmatrix}}^{\bar{A}} x + \begin{bmatrix} 1 \\ 0 \\ 0 \end{bmatrix} u$$
$$y = \begin{bmatrix} 0 & 0 & 0.5 \end{bmatrix} x$$

and removing $\bar{\delta}$ to get the healthy matrix of system A with the transfer function of the healthy system is defined as follows,

$$\Phi_{\mathcal{H}}(s) = \frac{0.375}{s^3 + 2.5s^2 + 1.75s + 0.375}$$

and for the unhealthy, it is given by,

$$\Phi_{\upsilon}(s) = \frac{0.375}{s^3 + (2.5 + \bar{\delta})s^2 + (1.75 + \bar{\delta})s + 0.375 + 0.25\bar{\delta}}$$

From the transfer functions created in Eqs. (13) and (14), the stability properties can be examined. For the healthy system, since δ_i and ψ_i are positive constants, the poles of the $\det(sI - A)$ are all negative so that the system is,

$$\det(sI - A) = (s + 0.5)(s + 1.5)(s + 0.5)$$

asymptotically stable, whereas for the faulty system with $\bar{\delta}$ as positive scalar with $\bar{\delta} > 0$ constitutes also asymptotically stable, such that

$$\det(sI - A) = (s + 0.5)\left(s + 1.5 + \bar{\delta}\right)(s + 0.5)$$

The controllablity matrices of the two conditions are illustrated as in Eqs. $(21a)$ and $(21b)$, such that

$$\mathcal{Q}_C(\mathcal{H}) = \begin{bmatrix} 1 & -0.5 & 0.25 \\ 0 & 0.5 & -1.00 \\ 0 & 0.0 & 0.75 \end{bmatrix}$$
$$\mathcal{Q}_C(\upsilon) = \begin{bmatrix} 1 & -0.5 & 0.25 \\ 0 & 0.5 & -1 - 0.5\bar{\delta} \\ 0 & 0.0 & 0.75 \end{bmatrix}$$

where the ranks of both $\mathcal{Q}_C(\mathcal{H})$ and $\mathcal{Q}_C(\upsilon)$ are $n = 3$ with $\bar{\delta} > 0$. Moreover, the observability matrices of both kind of systems are presented from Eqs. $(23a)$ and $(23b)$ as follows,

$$\mathcal{Q}_O(\mathcal{H}) = \begin{bmatrix} 0.000 & 0.000 & 0.500 \\ 0.000 & 0.750 & -0.250 \\ 0.375 & -1.500 & 0.125 \end{bmatrix}$$
$$\mathcal{Q}_O(\upsilon) = \begin{bmatrix} 0.000 & 0.000 & 0.500 \\ 0.000 & 0.750 & -0.250 \\ 0.375 & -1.5 - 0.75\bar{\delta} & 0.125 \end{bmatrix}$$

with the full rank for either two matrices $\rho_O = 3$. Recalling to Eqs. (25a) and (25b) with respect to estimation, the set matrices are

$$A_o = \begin{bmatrix} 0 & 0 & -0.375 \\ 1 & 0 & -1.750 \\ 0 & 1 & -2.500 \end{bmatrix}, \quad B_o = \begin{bmatrix} 1 \\ 0 \\ 0 \end{bmatrix}, \quad C_o = \begin{bmatrix} 0 & 0 & 1 \end{bmatrix}$$

such that the canonical form of its observability $\bar{\mathcal{Q}}_O$ along with the transformation matrix Δ is

$$\bar{\mathcal{Q}}_O = \begin{bmatrix} 0.0 & 0.0 & 1.0 \\ 0.0 & 1.0 & -2.5 \\ 1.0 & -2.5 & 4.5 \end{bmatrix}, \quad \Delta = \begin{bmatrix} \frac{8}{3} & -\frac{4}{3} & \frac{2}{3} \\ 0 & \frac{4}{3} & -\frac{8}{3} \\ 0 & 0 & 2 \end{bmatrix}$$

where the error dynamics defined as Γ is then resulted in the following,

$$\Gamma = \begin{bmatrix} 0 & 0 & -0.375 - l_1 \\ 1 & 0 & -1.750 - l_2 \\ 0 & 1 & -2.500 - l_3 \end{bmatrix}$$

so that the characteristic polynomial of the error Γ is matched to desired eigenvalues of λ_i. These desired poles are $\lambda_i, 1 \rightarrow 3$, comprising $-5, -8$, and -10, such that

$$\det(sI - \Gamma) = \det \begin{bmatrix} s & 0 & 0.375 + l_1 \\ -1 & s & 1.750 + l_2 \\ 0 & -1 & s + 2.500 + l_3 \end{bmatrix}$$

yielding,

$$s^3 + (2.5 + l_3)s^2 + (1.75 + l_2)s + (0.375 + l_1)$$

Those desired poles create the polynomial $\alpha_d = s^3 + 23s^2 + 170s + 400$ which is then compared to the above result. The following is to obtain the Ψ_o Eq. (28) leading to the observer gain Ψ as denoted in Eq. (29), therefore

$$\Psi_o = \begin{bmatrix} 399.625 \\ 168.250 \\ 20.500 \end{bmatrix}, \quad \Psi = \begin{bmatrix} 855 \\ 169.667 \\ 41 \end{bmatrix}$$

Finally, the dynamic of the system could be written as Γ_d using the information of the matrices of A, Ψ, and C as given,

$$\Gamma_d = \begin{bmatrix} -0.5 & 0.0 & -855.000 \\ 0.5 & -1.5 & -169.667 \\ 0.0 & 1.5 & -41.500 \end{bmatrix}$$

and moving to the output residual, since it is assumed that $\frac{1}{4} < x_i(0) \leq 4$ with $i = 1 \rightarrow 3$, the initial value being allowed in the estimation is $\hat{x}_i(0) = \frac{1}{4}$. From this, it can be concluded that the largest possible (upper-bound) value of the initial error $\hat{e}$ throughout the states is

$$\hat{e} = 4 - \frac{1}{4} = \frac{15}{4}$$

with the information in Eq. (31), the upper-bound residual of the output is given below, such that

$$\bar{\varepsilon}(t) = \frac{78}{64}e^{-5t} - \frac{765}{64}e^{-8t} + \frac{807}{64}e^{-10t} \tag{54}$$

Since this upper-bound shows the actual time of the residual with the condition of $x_i(0) = 4$, the detection threshold $\varepsilon(t)$ should be design larger than that actual function $\bar{\varepsilon}(t)$ so as to maintain the failure detection. Thus, the larger upper-bound of $\bar{\varepsilon}$(t) is

$$\bar{\varepsilon}(t) = \frac{78}{64}e^{-5t} + \frac{765}{64}e^{-8t} + \frac{807}{64}e^{-10t} \tag{55}$$

which is able to set as the detection threshold.

IV. SIMULATION AND FINDINGS

The following is to present the simulation results certain input $u(t)$ and $f(t)$ as in Eq. (3), such that,

$$u(t) = \begin{cases} 2, & 0 \leq t \leq 1 \\ \\ 1, & t \geq 1 \end{cases}$$

with three different initial conditions x_0 which is used as a comparison apart from the estimation methods,

$$\begin{bmatrix} x_0(1) \\ x_0(2) \\ x_0(3) \end{bmatrix} = \begin{bmatrix} 0.26 & 0.26 & 0.26 \\ 4 & 4 & 4 \\ 2.4 & 3.6 & 1.8 \end{bmatrix}$$

The design of gain observer along with two different estimation algorithms is compared in order to examine the ability to track with respect to MSE. Finally, the threshold design $\bar{\varepsilon}$ and residual output ε is implemented to show where the fault is detected, questioning the $\bar{\delta}$ at $t_f \geq 2$. Fig. (2a) presents the time behaviour of the state x_1 being affected by some initial conditions x_0 along with $u(t)$. Since there is no effect on the fault f, the response converges to the point of steady state. Due to the fault f disturbance on the second tank x_2, the values plummet as soon as the fault is occurring at $t_f = 2s$. The changes in input $u(t)$ in x_2 seems no impact compared to that of x_1. x_3 which is free from the continuity of the fault also converges to the same point as x_1, showing the positive response of $u(t)$.

It can be deduced that x_0 yields divergent transient of $\hat{x}$ because of the error steady state of $e(0) = x(0) - \hat{x}(0)$ with respect to certain initial conditions. Nevertheless, the steady states throughout x cannot be said as the influence of x_0. Fig. (2d), (2e), (2f) performs three different responses due to three various x_0 with disturbance observer. Compared to them, Fig. (2g), (2h), (2i) implement adaptive-Kalman showing slightly divergent outcome which are better than that of consensus filtering. Fig. (2j), (2k), and (2l) define the different fault detection where the output residual starts to overtake the threshold, meaning the fault is detected. From three $x_0(1), x_0(2), x_0(3)$, it results in $2.0235, 2.015$, and 2.0165 respectively as the intersection between those two parameters, writing as $|\varepsilon(t_d)| > \bar{\varepsilon}(t_d)$. This can be summarized that the output residual would be relatively small for $t < t_f$ in comparison with the threshold. Due to the coincidence points after the transient observer, the time required to intersect the threshold is just slightly after the occurrence of the fault f.

V. CONCLUSION

The initial mathematical model of hydraulic system has been proposed along with the construction of stability properties. The estimation methods are applied with the Luenberger observer, adaptive-scaling Kalman, and consensus filtering to examine the unhealthy system. Fault detection scheme for certain time t_f is designed and tested mathematically and in simulation. The results show that the fault detection scenarios are successfully proposed.

http://dx.doi.org/10.29322/IJSRP.11.05.2021.p11308

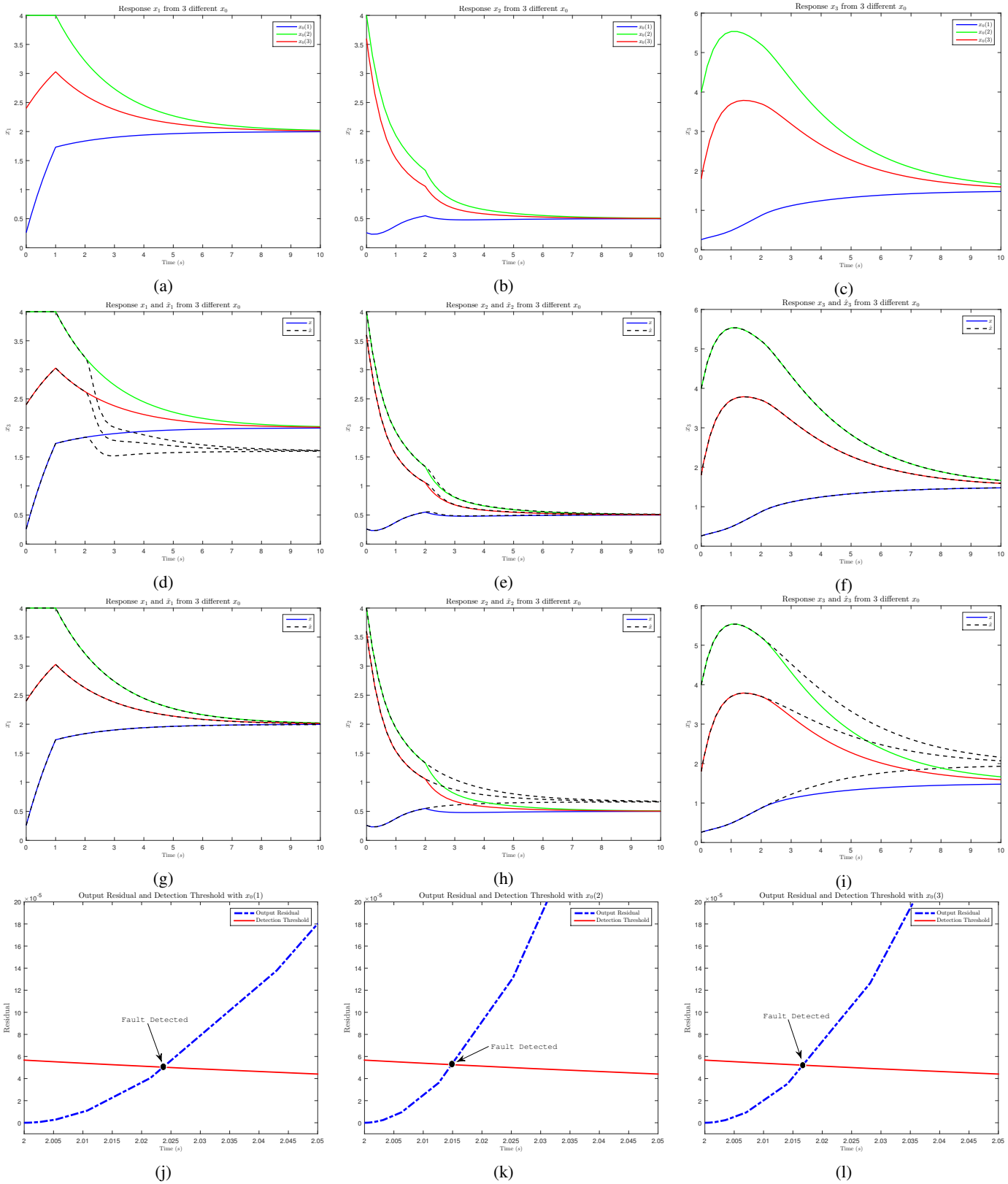

(a) (b) (c)

(d) (e) (f)

(g) (h) (i)

(j) (k) (l)

Fig. 2: Fig. 2a-2c Response variations from x_1, x_2, and x_3 due to three initial conditions $x_0(1)$, $x_0(2)$, and $x_0(2)$; Fig. 2d-2f The same scenarios with Luenberger observer; Fig. 2g-2i The same scenarios with Adaptive-Scaling Kalman; Fig. 2j-2l Fault detection from three divergent x_0

http://dx.doi.org/10.29322/IJSRP.11.05.2021.p11308

ACKNOWLEDGMENT

Thanks to Professor Thomas Parisini from the Imperial College London who has taught me in the lecture leading to finishing this paper and to LPDP (Indonesia Endowment Fund for Education) Scholarship from Indonesia.

REFERENCES

[1] Dingli Yu, D. N. Shields, and J. L. Mahtani, "A nonlinear fault detection method for a hydraulic system," in *1994 International Conference on Control - Control '94.*, vol. 2, March 1994, pp. 1318–1322 vol.2.

[2] P. Bistk, "Identification and control of hydraulic system using visual feedback," in *2016 International Conference on Emerging eLearning Technologies and Applications (ICETA)*, Nov 2016, pp. 29–34.

[3] N. Helwig, S. Klein, and A. Schtze, "Identification and quantification of hydraulic system faults based on multivariate statistics using spectral vibration features," *Procedia Engineering*, vol. 120, pp. 1225 – 1228, 2015, eurosensors 2015.

[4] S. Vsquez, M. Kinnaert, and R. Pintelon, "Active fault diagnosis on a hydraulic pitch system based on frequency-domain identification," *IEEE Transactions on Control Systems Technology*, vol. 27, no. 2, pp. 663–678, March 2019.

[5] F. Wang and Y. Chen, "Dynamic characteristics of pressure compensator in underwater hydraulic system," *IEEE/ASME Transactions on Mechatronics*, vol. 19, no. 2, pp. 777–787, April 2014.

[6] S. Gayaka and B. Yao, "Fault detection, identification and accommodation for an electro-hydraulic system: An adaptive robust approach," *IFAC Proceedings Volumes*, vol. 41, no. 2, pp. 13 815 – 13 820, 2008, 17th IFAC World Congress.

[7] S. Sharifi, A. Tivay, S. M. Rezaei, M. Zareinejad, and B. Mollaei-Dariani, "Leakage fault detection in electro-hydraulic servo systems using a nonlinear representation learning approach," *ISA Transactions*, vol. 73, pp. 154 – 164, 2018.

[8] G. Shen, Z. Zhu, J. Zhao, W. Zhu, Y. Tang, and X. Li, "Real-time tracking control of electro-hydraulic force servo systems using offline feedback control and adaptive control," *ISA Transactions*, vol. 67, pp. 356 – 370, 2017.

[9] Z. MA, S. WANG, J. SHI, T. LI, and X. WANG, "Fault diagnosis of an intelligent hydraulic pump based on a nonlinear unknown input observer," *Chinese Journal of Aeronautics*, vol. 31, no. 2, pp. 385 – 394, 2018.

[10] K. Vereide, B. Svingen, T. K. Nielsen, and L. Lia, "The effect of surge tank throttling on governor stability, power control, and hydraulic transients in hydropower plants," *IEEE Transactions on Energy Conversion*, vol. 32, no. 1, pp. 91–98, March 2017.

[11] D. Angeli, "A lyapunov approach to incremental stability properties," *IEEE Transactions on Automatic Control*, vol. 47, no. 3, pp. 410–421, March 2002.

[12] D. Nesic and A. R. Teel, "Input-output stability properties of networked control systems," *IEEE Transactions on Automatic Control*, vol. 49, no. 10, pp. 1650–1667, Oct 2004.

[13] Y. Huang, Y. Zhang, B. Xu, Z. Wu, and J. A. Chambers, "A new adaptive extended kalman filter for cooperative localization," *IEEE Transactions on Aerospace and Electronic Systems*, vol. 54, no. 1, pp. 353–368, Feb 2018.

[14] V. Lippiello, B. Siciliano, and L. Villani, "Adaptive extended kalman filtering for visual motion estimation of 3d objects," *Control Engineering Practice*, vol. 15, no. 1, pp. 123 – 134, 2007.

[15] S. Roujol, B. Denis de Senneville, S. Hey, C. Moonen, and M. Ries, "Robust adaptive extended kalman filtering for real time mr-thermometry guided hifu interventions," *IEEE Transactions on Medical Imaging*, vol. 31, no. 3, pp. 533–542, March 2012.

[16] M. Efe, J. A. Bather, and D. P. Atherton, "An adaptive kalman filter with sequential rescaling of process noise," in *Proceedings of the 1999 American Control Conference (Cat. No. 99CH36251)*, vol. 6, June 1999, pp. 3913–3917 vol.6.

[17] V. A. Bavdekar, R. B. Gopaluni, and S. L. Shah, "Evaluation of adaptive extended kalman filter algorithms for state estimation in presence of model-plant mismatch," *IFAC Proceedings Volumes*, vol. 46, no. 32, pp. 184 – 189, 2013, 10th IFAC International Symposium on Dynamics and Control of Process Systems.

[18] R. Olfati-Saber, "Distributed kalman filter with embedded consensus filters," in *Proceedings of the 44th IEEE Conference on Decision and Control*, Dec 2005, pp. 8179–8184.

[19] M. K. Wafi, "Filtering module on satellite tracking," *AIP Conference Proceedings*, vol. 2088, no. 1, p. 020045, 2019.